Perovskite Phases

International Edition: DOI: 10.1002/anie.201506456
German Edition: DOI: 10.1002/ange.201506456

Giant Magnetoresistance in the Half-Metallic Double-Perovskite Ferrimagnet Mn_2FeReO_6

*Man-Rong Li, Maria Retuerto, Zheng Deng, Peter W. Stephens, Mark Croft, Qingzhen Huang, Hui Wu, Xiaoyu Deng, Gabriel Kotliar, Javier Sánchez-Benítez, Joke Hadermann, David Walker, and Martha Greenblatt**

Abstract: *The first transition-metal-only double perovskite compound, $Mn^{2+}{}_2Fe^{3+}Re^{5+}O_6$, with 17 unpaired d electrons displays ferrimagnetic ordering up to 520 K and a giant positive magnetoresistance of up to 220% at 5 K and 8 T. These properties result from the ferrimagnetically coupled Fe and Re sublattice and are affected by a two-to-one magnetic-structure transition of the Mn sublattice when a magnetic field is applied. Theoretical calculations indicate that the half-metallic state can be mainly attributed to the spin polarization of the Fe and Re sites.*

Perovskite oxides with unpaired d electrons present scientifically and practically interesting electronic and magnetic properties.[1–3] Recently, renewed interest has been focused on the $A_2BB'O_6$ double perovskites (A = alkaline earth or rare earth metal or Pb; B/B′ = transition metals such as Fe/Mo and Fe/Re) because of their colossal magnetoresistance (CMR) and half-metallic (HM) properties, which are potentially useful for spintronic applications.[2,4–6] The crystal structures and physical properties of these materials can be effectively manipulated by controlling the size of the A site cations.[7] Perovskites with unusually small A site cations are an emerging field for exotic properties,[8] especially when transition-metal ions with unpaired d electrons are incorporated into the A site for an improved performance.[9] Generally, these materials can only be prepared at high pressure and temperature (HPT), and owing to their small tolerance factors (t), the perovskite structures compete with corundum-related structures.[10–14] To the best of our knowledge, only three $ABO_3/A_2BB'O_6$ type perovskites, namely $MnVO_3$ (*Pnma*, antiferromagnetic (AFM) metal)[9,15] and Mn_2MSbO_6 (M = Fe and Cr),[16,17] have been prepared with transition-metal ions at both the A and B sites. The perovskite polymorphs $Mn^{2+}{}_2M^{3+}Sb^{5+}O_6$ ($P2_1/n$) can be prepared at 5 (M = Fe) and 8 GPa (M = Cr) with M^{3+} and Sb^{5+} ordered at the B and B′ sites. Although high-spin (HS) d^5 Mn^{2+} and Fe^{3+} and d^3 Cr^{3+} ions occupy the A and B sites in Mn_2MSbO_6, their properties are not so remarkable (AFM insulators with $T_N \approx 60$ and 55 K for M = Fe and Cr, respectively), likely because of the non-magnetic Sb^{5+} ion at the B′ site. Therefore, the incorporation of transition-metal ions at all of the cation sites in $A_2BB'O_6$ was anticipated to result in unusual properties. Herein, we report the first transition-metal-ion-only double perovskite oxide Mn_2FeReO_6, which was synthesized by an HPT method. The crystal and magnetic structures as well as the magnetotransport properties were experimentally and theoretically investigated in detail.

Polycrystalline Mn_2FeReO_6 was prepared at 1623 K under 5 GPa. Energy-dispersive X-ray spectroscopy gave a composition of $Mn_{1.98(10)}Fe_{0.98(7)}Re_{1.04(16)}O_x$, which is in good agreement with the nominal composition. The room temperature (RT) powder X-ray diffraction (PXD) patterns of Mn_2FeReO_6 indicate a pure phase with a monoclinic or orthorhombic cell (Supporting Information, Figure S1 a), but it is difficult to determine the space group (SG) owing to the small deviation of the monoclinic angle from 90°. This as-made phase was stable up to 850 K upon heating at ambient pressure, at which point it decomposed (Figure S1 b). Subsequent electron diffraction experiments confirmed the cell dimensions (Figure S2) and suggested a monoclinic $P2_1/n$ (No. 14), or orthorhombic Pn type [$Pnm2_1$ or $Pn2_1m$ (No. 31) or $Pnmm$ (No. 59)] SG. Finally, the crystal structure was conclusively determined to be monoclinic $P2_1/n$ by high-resolution synchrotron PXD (SPXD) data refinements

[*] Dr. M. R. Li, Dr. M. Retuerto, Z. Deng, Prof. M. Greenblatt
Department of Chemistry and Chemical Biology
Rutgers, The State University of New Jersey
610 Taylor Road, Piscataway, NJ 08854 (USA)
E-mail: martha@rutchem.rutgers.edu
Dr. M. Retuerto
Niels Bohr Institute, University of Copenhagen
2100 Copenhagen (Denmark)
Dr. P. W. Stephens
Department of Physics & Astronomy
State University of New York
Stony Brook, NY 11794 (USA)
Dr. M. Croft, X. Deng, G. Kotliar
Department of Physics & Astronomy
Rutgers, The State University of New Jersey
136 Frelinghuysen Road, Piscataway, NJ 08854 (USA)
Dr. Q. Huang, H. Wu
Center for Neutron Research
National Institute of Standards and Technology (NIST)
Gaithersburg, MD 20899-6102 (USA)
Dr. J. Sánchez-Benítez
Departamento de Química Física I, Facultad de Ciencias Químicas
Universidad Complutense de Madrid
28040 Madrid (Spain)
Dr. J. Hadermann
EMAT, University of Antwerp
Groenenborgerlaan 171, 2020 Antwerp (Belgium)
Dr. D. Walker
Lamont-Doherty Earth Observatory, Columbia University
61 Route 9W, Palisades, NY 10964 (USA)

Supporting information for this article is available on the WWW under http://dx.doi.org/10.1002/anie.201506456.

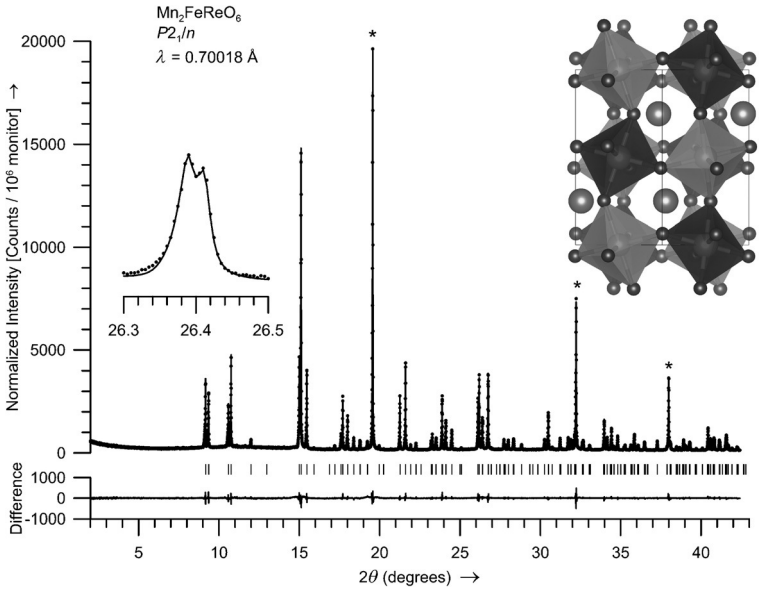

Figure 1. Rietveld refinement of the SPXD data for Mn_2FeReO_6 in the monoclinic $P2_1/n$ structure at RT. Asterisks indicate peaks from diamond diluent (internal standard) accounting for 90% of the sample by weight. Tick marks indicate the positions of allowed perovskite-phase peaks. The left inset shows the monoclinic splitting of the (204) reflection. The right inset shows the crystal structure viewed along [110] direction. Mn ions are shown as large spheres, O ions as small spheres, and the FeO_6 and ReO_6 octahedra are light and dark gray, respectively.

(Figure 1; $a = 5.20098(2)$, $b = 5.36399(2)$, $c = 7.58904(3)$ Å, $\beta = 89.95(1)°$, $V = 211.719(1)$ Å^3, $R_p/R_{wp} = 5.50/7.08\,\%$, $\chi^2 = 1.65$). Approximately 5(1) % of Fe and Re anti-site disorder was observed, giving a compositional formula of $Mn_2(Fe_{0.95(1)}Re_{0.05(1)})(Re_{0.95(1)}Fe_{0.05(1)})O_6$. The refined structural parameters and agreement factors are listed in Table S1, and selected interatomic distances and bond angles are given in Table S2. Mn_2FeReO_6 crystallizes in a highly distorted double-perovskite structure, where the Mn cations are coordinated by eight oxygen atoms, and corner-sharing FeO_6 and ReO_6 octahedra are rock-salt-ordered over the B and B′ sites (Figure 1, inset). It is isostructural with Ca_2FeReO_6[7] and Mn_2FeSbO_6,[18] and consistent with the *t*-dependent structural evolution law for A_2FeReO_6 (A = alkali earth) complexes shown in Figure S3. The size of the Mn^{2+} ions at the A positions is extremely small for a perovskite and forces the FeO_6 and ReO_6 octahedra to tilt in order to optimize the Mn–O distances. The tilting angle was estimated using the parameter $\Phi = (180° - \theta)/2$ where θ is the average angle of Fe1/Re1-O-Fe2/Re2. In Mn_2FeReO_6, this angle is 140.63° (Table S2), and therefore $\Phi = 19.7°$, which indicates a significantly higher distortion than in other distorted perovskites, such as Ca_2CrSbO_6, where the A cation is bigger and $\Phi = 13.5°$.[19] The Mn–O distances with eightfold coordination (2.379(10) Å at room temperature; Table S2) are also smaller than other A–O distances in distorted double perovskites, such as Ca_2FeReO_6 (Ca–O = 2.499(3) Å).[20] Bond valence sum (BVS, Table S2) calculations[21] suggested formal oxidation states of $Mn^{2+}{}_2Fe^{3+}Re^{5+}O_6$, which was confirmed by X-ray absorption near-edge spectroscopy (XANES; Figure S4–S6).

Temperature-dependent magnetic susceptibility [$\chi(T)$] measurements were performed between 5 and 600 K (Figure 2a). In the low-temperature regime (5–400 K; see Figure 2a, i), the measurements were conducted by both zero field cooling (ZFC) and field cooling (FC). The ZFC and FC curves diverge below 400 K owing to the competition between different magnetic interactions, as might be expected for a system with so many magnetic ions. A high ferromagnetic T_C of approximately 520 K was observed. Above T_C, the reciprocal susceptibility slightly deviated from linear behavior with a parabolic shape, which is also a typical ferromagnetic behavior. A regular Curie–Weiss (CW) law was adopted for a good fit in the range of 530–600 K (Figure 2a, ii). The paramagnetic temperature ($\theta = 502$ K) is close to the T_C observed, which indicates that ferro- or ferrimagnetic interactions are predominant. The paramagnetic effective moment ($\mu_{eff} = 4.4\,\mu_B$/f.u.; f.u. = formula unit) is much smaller than the expected value ($10.6\,\mu_B$/f.u.). The large difference between the observed and expected μ_{eff} values may be attributed to possible short-range order above T_C, which affects the correct evaluation of $\chi(T)$, or to spin–orbit coupling, which has been reported to have an effect on μ_{eff} for Re-based perovskites.[22,23]

The hysteresis loops indicate clear ferromagnetic behavior (Figure 2b). At 5 K, the saturation magnetization (μ_s) of $4.9\,\mu_B$/f.u. indicates ferrimagnetic (FiM) ordering of the cations, as it is much lower than the theoretical sum of the spin-only moments ($17\,\mu_B$/f.u.). Unlike for the A_2FeMoO_6 family, where the large Fe-O-Mo bond angle deviation from 180° for smaller A cations reduces the dpd π coupling and decreases T_C, the Re analogues show the highest T_C for the smaller A cations, which was attributed to the strong spin–orbit coupling of the 5d transition metals,[24] giving a T_C value of 520 K for Mn_2FeReO_6, which is comparable with that of Ca_2FeReO_6 (ca. 530 K).[7]

Interestingly, Mn_2FeReO_6 is more insulating than other A_2FeReO_6 (A = alkali earth or Pb) phases, where the resistivity (ρ) varies between 0.05 and 1 Ω cm at RT,[7,25] considering that Mn_2FeReO_6 has a greater number of unpaired d electrons. Figure 3 shows the temperature dependence of the ρ value of Mn_2FeReO_6 at zero field and 8 T. The resistivity values are almost identical above 150 K at 0 and 8 T, with $\rho = 4.98$ (0 T) and 4.97 (8 T) Ω cm at RT, indicating the absence of magnetoresistance (MR) at higher temperatures. The ρ value increases slowly down to 50 K, and below 50 K, the resistivity increases steeply with decreasing temperature. The small anomaly around 50 K is probably due to magnetoelastic coupling, which is also observed in other Re perovskites (Ca_2FeReO_6)[7] and has been reported to be related to Re spin–orbit coupling that couples the magnetic moment with the lattice, as also supported by the lattice parameter evolution (Figure S7). At 5 K, the resistivity values increase to 122.58 and 396.32 Ω cm at 0 and 8 T, respectively, which corresponds to a positive MR of approximately 220 %. The isothermal MR ratio between −8 and 8 T at 5 K, with

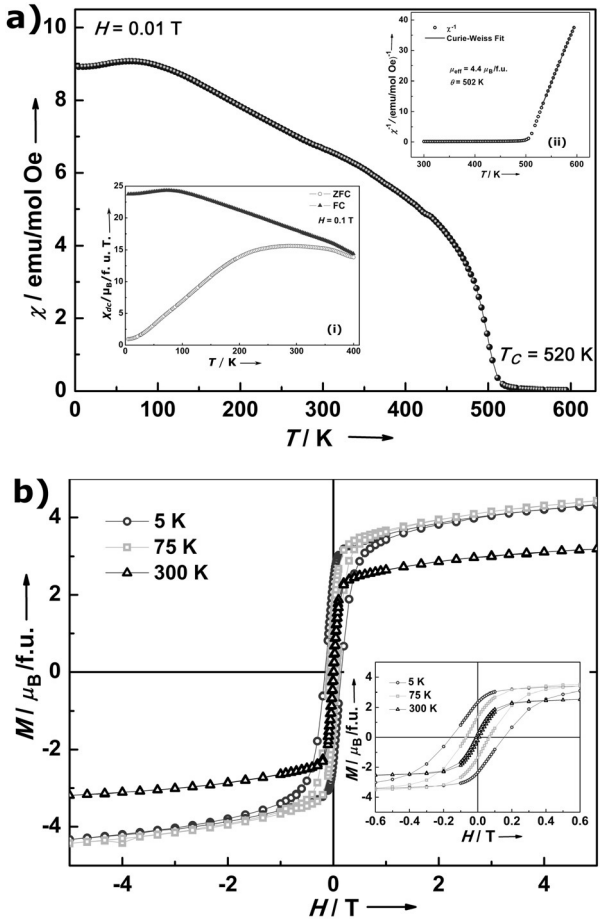

Figure 2. a) The $\chi(T)$ curves up to 600 K show the magnetic transition temperature (T_C) of 520 K. i) ZFC and FC data up to 400 K. ii) The inverse susceptibility (χ^{-1}) versus temperature curve nicely fits to the CW model over the paramagnetic region. b) Isothermal magnetization curves at 5, 75, and 300 K between −5 and 5 T. Inset: Enlarged area between −0.6 and 0.6 T.

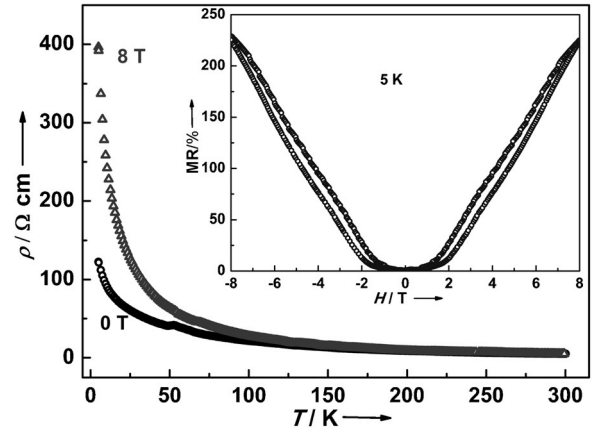

Figure 3. Temperature-dependent resistivity of Mn_2FeReO_6 at zero field and 8 T. Inset: The isothermal MR ratio between −8 and 8 T at 5 K, with the maximum positive MR ratio of approximately 220% at 8 T.

a slim butterfly-like shape, is shown in the inset in Figure 3. Unlike other A_2FeMO_6 (M = Mo and Re) materials with a negative MR ratio of approximately −15%, the MR of Mn_2FeReO_6 is positive and much larger.

Powder neutron diffraction (PND) data, collected with and without an applied magnetic field at different temperatures, were obtained to determine the magnetic structures and to better understand the giant positive MR in Mn_2FeReO_6 (Figure S8 and Tables S3 and S4). The magnetic structures at low temperature (4 and 70 K) and 0 T have to be explained in terms of two different AFM structures: one for the Mn cations and another one for the FiM arrangement of the Fe and Re moments. At 4 K and 0 T, the Mn moments are aligned antiferromagnetically along the x and z directions ($m_x = 2.05(11)\,\mu_B$, $m_z = 1.3(2)\,\mu_B$), and the y component is equal to zero in one magnetic structure (Figure 4a, left),

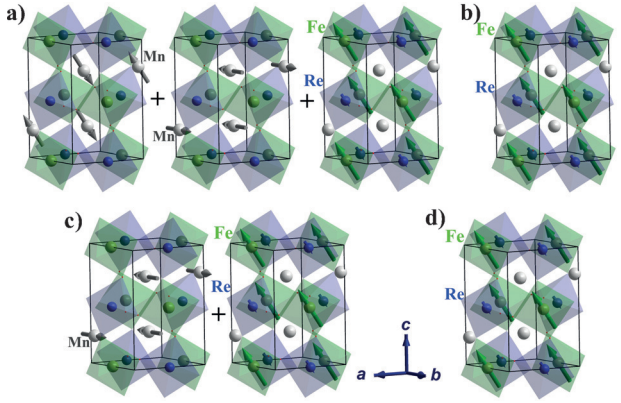

Figure 4. Magnetic structures of Mn_2FeReO_6 a) at 4 K and 0 T with two AFM-coupled Mn sublattices and FiM spin alignment of the Fe/Re lattice, b) at 250 K and 0 T with FiM ordering of Fe and Re, c) at 4 K and 7 T with an AFM-coupled Mn lattice and a FiM Fe and Re arrangement, and d) at 250 K and 7 T with a FiM Fe and Re lattice.

whereas the other magnetic structure (Figure 4a, middle) has x and z components equal to zero, and only the y AFM component deviates from zero (Mn $m_y = -2.91\,\mu_B$). Therefore, the magnetic structure of Mn is represented by two different sublattices with all of the components coupled antiferromagnetically, and cannot be explained with one single magnetic structure because this would correspond to a forbidden solution for its monoclinic space group. In the case of Fe and Re, the Fe and Re moments are $m_x = m_z = 3.19(8)\,\mu_B$ and $m_x = m_z = -0.143(3)\,\mu_B$, respectively, and the components along the y axis are again zero; the Fe and Re spins are antiparallel and form a net FiM structure (Figure 4a, right), which can be defined as a $P2_1/m$ magnetic space group. The coexistence of two different Mn AFM structures and the FiM Fe/Re magnetic structure can account for the high resistivity of Mn_2FeReO_6 compared to similar phases with non-transition-metal ions at the A sites.

The magnetic structure at 70 K and $H = 0$ T is the same as that at 4 K and $H = 0$ T, but with smaller magnetic moments (Table S3). At 250 or 300 K and 0 T, the Fe and Re moments correspond to the same FiM structure as at 4 K and $H = 0$ T, but are smaller, while the Mn cations are no longer magnetically ordered (Table S3 and Figure 4b). To the best of our knowledge, only Sr_2CoOsO_6 has been established to feature

two interpenetrating magnetic sublattices with clearly different and independent ordering magnetic transitions among the double perovskites.[26] As the Mn sublattice is no longer magnetically ordered at high temperature, it cannot affect the Fe and Re magnetic sublattice, and the resistance of the sample decreases compared to that at 4 K (Figure 4a). At 7 T and 4 K, the simultaneous presence of two different magnetic sublattices that defined the Mn magnetic structure at $H = 0$ T is no longer valid. The second AFM Mn structure (Figure 4a, middle), together with the FiM sublattice of the Fe and Re cations, can be used to explain the data (Figure S8c): The applied magnetic field (7 T) brings about a transition that simplifies the magnetic structure. The magnetic moments of Mn are now AFM-coupled and oriented along the y axis ($m_y = -2.93(5)\,\mu_B$), as the components along the x and z directions become zero (Figure 4c and Table S4). The FiM Fe/Re sublattice gives a net magnetic moment of 5.0 μ_B, which is similar to the saturation magnetization (4.9 μ_B) at 5 K and 5 T (see Figure 2b). We propose that this magnetic structure at 4 K and 7 T hinders the half-metallicity of sublattice B more than the combination of magnetic structures found at 0 T, which could explain the incremental change in the resistivity when a magnetic field is applied. At 250 K and 7 T, the magnetic structure (Figure 4d and Table S4) is similar to that at 250 K and 0 T (Figure 4b). These magnetic-structure evolutions are also reflected by the PND patterns in Figure S9. When an external magnetic field is applied, the orientation of the spin and orbital moments of Re could be modified in a way that hinders the half-metallicity and increases the global resistivity of the material. Other Re double perovskites, Ba_2MnReO_6, and Ca_2FeReO_6 have been reported to present positive MR,[27,28] but with much smaller values.

First-principle calculations based on density functional theory (DFT) can stabilize a collinear magnetic structure of Mn_2FeReO_6, which correctly captures the AFM and FiM coupling of the Mn and Fe/Re sublattices, respectively. The corresponding density of states (DOS) and the electronic band structure are shown in Figures 5 and S10. Both the Mn and Fe sites are nearly fully polarized by a large exchange splitting between the spin majority and minority components, while the Re site is weakly polarized with a much smaller exchange splitting. The scenario is in agreement with the PND measurements, where large moments were observed for the Mn and Fe sites and a much smaller moment for the Re site. Interestingly, the DOS exhibits a significant insulating gap (ca. 1.0 eV) in the spin majority component and a relatively high density of states in the spin minority component at the Fermi level; thus the pronounced HM behavior is mainly due to the Re and Fe sites. Therefore, it is likely that the half-metallicity of the Fe/Re sublattice is affected by the complicated magnetic structure of the Mn sites in a way that an external magnetic field would modify the electronic structure to produce the observed giant positive MR. It is also possible that the spin–orbit coupling of the Re moments has an effect on the positive MR, but this point needs further clarification.

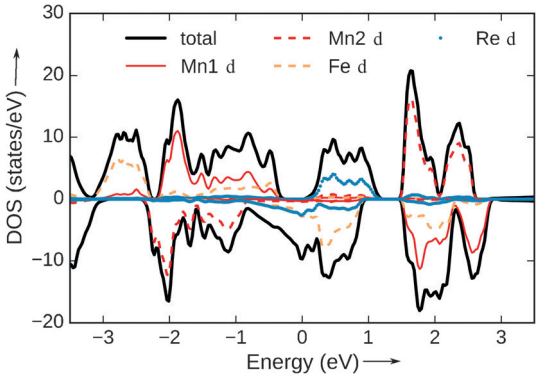

Figure 5. The computed DOS of Mn_2FeReO_6 and its projections onto the d orbitals of different sites. Positive (negative) values corresponds to spin majority (minority) components.

In conclusion, the first transition-metal-only double perovskite compound, Mn_2FeReO_6, has been prepared at high pressure and temperature, and was experimentally and theoretically established to be a half-metallic ferrimagnet ($T_C = 520$ K) above room temperature with giant positive magnetoresistance (ca. 220 %). These findings set a record for the number of unpaired d electrons (17) in a double perovskite oxide and will encourage further searches for new multifunctional materials.

Experimental Section

Experimental details, electron-diffraction and crystal-structure data, XANES, detailed powder neutron diffraction data analysis, low-temperature lattice parameter evolution, and theoretical calculations are presented in the Supporting Information. Further details on the crystal structure investigation may be obtained from the Fachinformationszentrum Karlsruhe, 76344 Eggenstein-Leopoldshafen, Germany (fax: (+49) 7247-808-666; e-mail: crysdata@fiz-karlsruhe.de), quoting the depository numbers CSD429762 to 429768.

Acknowledgements

This work was supported by NSF-DMR-0966829 and ARO-434603 (DOD-VV911NF-12-1-0172) grants. X.D. and G.K. are supported by the NSF-DMREF project DMR-1435918. J.S.-B. is supported by the Spanish projects MAT2013-41099-R and RyC-2010-06276. M.R. is supported by the Danish Research Councils for Independent Research (12-125226). Use of the NSLS, Brookhaven National Laboratory was supported by the DOE BES (DE-AC02-98CH10886). We would like to thank J. Hanley at LDEO, Columbia University for making the high-pressure assemblies, and Dr. Tapati Sarkar at Uppsala University for the original magnetism check.

Keywords: density functional calculations · giant magnetoresistance · half-metallicity · magnetic properties · perovskite phases

How to cite: *Angew. Chem. Int. Ed.* **2015**, *54*, 12069–12073
Angew. Chem. **2015**, *127*, 12237–12241

[1] J. M. D. Teresa, M. R. Ibarra, P. A. Algarabel, C. Ritter, C. Marquina, J. Blasco, J. Garcia, A. del Moral, Z. Arnold, *Nature* **1997**, *386*, 256 – 259.
[2] K. I. Kobayashi, T. Kimura, H. Sawada, K. Terakura, Y. Tokura, *Nature* **1998**, *395*, 677.
[3] J. B. Goodenough, *Chem. Mater.* **2013**, *26*, 820 – 829.
[4] R. A. de Groot, F. M. Mueller, P. G. van Engen, K. H. J. Buschow, *Phys. Rev. Lett.* **1983**, *50*, 2024 – 2027.
[5] K. I. Kobayashi, T. Kimura, Y. Tomioka, H. Sawada, K. Terakura, Y. Tokura, *Phys. Rev. B* **1999**, *59*, 11159 – 11162.
[6] D. Serrate, J. M. D. Teresa, M. R. Ibarra, *J. Phys. Condens. Matter* **2007**, *19*, 023201.
[7] J. M. De Teresa, D. Serrate, J. Blasco, M. R. Ibarra, L. Morellon, *Phys. Rev. B* **2004**, *69*, 144401.
[8] A. B. Alexei, Y. Wei, *J. Phys. Condens. Matter* **2014**, *26*, 163201.
[9] M. Markkula, A. M. Arevalo-Lopez, A. Kusmartseva, J. A. Rodgers, C. Ritter, H. Wu, J. P. Attfield, *Phys. Rev. B* **2011**, *84*, 094450.
[10] M.-R. Li, D. Walker, M. Retuerto, T. Sarkar, J. Hadermann, P. W. Stephens, M. Croft, A. Ignatov, C. P. Grams, J. Hemberger, I. Nowik, P. S. Halasyamani, T. T. Tran, S. Mukherjee, T. S. Dasgupta, M. Greenblatt, *Angew. Chem. Int. Ed.* **2013**, *52*, 8406 – 8410; *Angew. Chem.* **2013**, *125*, 8564 – 8568.
[11] M.-R. Li, P. W. Stephens, M. Retuerto, T. Sarkar, C. P. Grams, J. Hemberger, M. C. Croft, D. Walker, M. Greenblatt, *J. Am. Chem. Soc.* **2014**, *136*, 8508 – 8511.
[12] M.-R. Li, M. Retuerto, D. Walker, T. Sarkar, P. W. Stephens, S. Mukherjee, T. S. Dasgupta, J. P. Hodges, M. Croft, C. P. Grams, J. Hemberger, J. Sánchez-Benítez, A. Huq, F. O. Saouma, J. I. Jang, M. Greenblatt, *Angew. Chem. Int. Ed.* **2014**, *53*, 10774 – 10778; *Angew. Chem.* **2014**, *126*, 10950 – 10954.
[13] M.-R. Li, M. Croft, P. W. Stephens, M. Ye, D. Vanderbilt, M. Retuerto, Z. Deng, C. P. Grams, J. Hemberger, J. Hadermann, W.-M. Li, C.-Q. Jin, F. O. Saouma, J. I. Jang, H. Akamatsu, V. Gopalan, D. Walker, M. Greenblatt, *Adv. Mater.* **2015**, *27*, 2177 – 2181.
[14] R. Mathieu, S. A. Ivanov, G. V. Bazuev, M. Hudl, P. Lazor, I. V. Solovyev, P. Nordblad, *Appl. Phys. Lett.* **2011**, *98*, 202505.
[15] Y. Syono, S.-I. Akimoto, Y. Endoh, *J. Phys. Chem. Solids* **1971**, *32*, 243 – 249.
[16] R. Mathieu, S. A. Ivanov, I. V. Solovyev, G. V. Bazuev, P. Anil Kumar, P. Lazor, P. Nordblad, *Phys. Rev. B* **2013**, *87*, 014408.
[17] A. J. Dos santos-García, E. Solana-Madruga, C. Ritter, D. Avila-Brande, O. Fabelo, R. Saez-Puche, *Dalton Trans.* **2015**, *44*, 10665.
[18] A. P. Tyutyunnik, G. V. Bazuev, M. V. Kuznetsov, Y. G. Zainulin, *Mater. Res. Bull.* **2011**, *46*, 1247 – 1251.
[19] M. Retuerto, J. A. Alonso, M. García-Hernández, M. J. Martínez-Lope, *Solid State Commun.* **2006**, *139*, 19 – 22.
[20] K. Oikawa, T. Kamiyama, H. Kato, Y. Tokura, *J. Phys. Soc. Jpn.* **2003**, *72*, 1411 – 1417.
[21] I. D. Brown, *Chem. Rev.* **2009**, *109*, 6858 – 6919.
[22] A. Winkler, N. Narayanan, D. Mikhailova, K. G. Bramnik, H. Ehrenberg, H. Fuess, G. Vaitheeswaran, V. Kanchana, F. Wilhelm, A. Rogalev, A. Kolchinskaya, L. Alff, *New J. Phys.* **2009**, *11*, 073047.
[23] H. Wu, *Phys. Rev. B* **2001**, *64*, 125126.
[24] M. Sikora, C. Kapusta, M. Borowiec, C. J. Oates, V. Prochazka, D. Rybicki, D. Zajac, J. M. De Teresa, C. Marquina, M. R. Ibarra, *Appl. Phys. Lett.* **2006**, *89*, 062509.
[25] K. Nishimura, M. Azuma, S. Hirai, M. Takano, Y. Shimakawa, *Inorg. Chem.* **2009**, *48*, 5962 – 5966.
[26] R. Morrow, R. Mishra, O. D. Restrepo, M. R. Ball, W. Windl, S. Wurmehl, U. Stockert, B. Büchner, P. M. Woodward, *J. Am. Chem. Soc.* **2013**, *135*, 18824 – 18830.
[27] G. Popov, M. Greenblatt, M. Croft, *Phys. Rev. B* **2003**, *67*, 024406.
[28] D. Serrate, J. M. De Teresa, P. A. Algarabel, C. Marquina, L. Morellon, J. Blasco, M. R. Ibarra, *J. Magn. Magn. Mater.* **2005**, *290 – 291*, *Part 2*, 843 – 845.

Received: July 13, 2015
Published online: July 31, 2015

